EURASIP Journal on Wireless Communications and Networking

RESEARCH Open Access

Multi-user directional modulation with reconfigurable holographic surfaces

M. Yaser Yağan[1,2*], Samed Keşir[1], İbrahim Hökelek[1], Ali E. Pusane[2] and Ali Görçin[1,3]

*Correspondence:
yaser.yagan@tubitak.gov.tr

[1] Communications and Signal Processing Research (HİSAR) Laboratory, TÜBİTAK BİLGEM, 41470 Gebze, Kocaeli, Turkey
[2] Department of Electrical and Electronics Engineering, Boğaziçi University, 34342 İstanbul, Turkey
[3] Department of Electronics and Communication Engineering, Istanbul Technical University, 34485 İstanbul, Turkey

Abstract

Large intelligent surfaces arise as an emerging technology and critical building block for sixth-generation (6G) wireless networks. Reconfigurable holographic surfaces (RHSs) have been attracting significant attention recently as active antenna arrays with the capability of forming narrow beams at low cost and complexity. This paper introduces the directional modulation (DM) concept for RHS, where a large number of elements are exploited to control not only the signal's power at the receiver but also its phase. Thus, a novel DM algorithm is proposed for RHS enables modulating a carrier wave to transmit information toward specific directions while broadcasting arbitrary signals toward other directions. Error vector magnitude results are reported for multiple users, where the directions of two users with respect to the RHS are varied. Mutual information result is also provided for 6 users to demonstrate the application of RHS for the physical layer security. Results are highly promising for future low-cost and secure spatially multiplexed communications.

Keywords: Holographic beamforming, Directional modulation, Reconfigurable holographic surface

1 Introduction

Sixth-generation (6G) wireless communications boost the development of novel technologies toward creating an all-encompassing intelligent information network. Recent research has focused on boosting system capacity, decreasing latency, and enhancing connectivity to meet these needs and improve overall performance. Massive multiple input multiple output (mMIMO) and millimeter wave (mmWave) communications have both come to be acknowledged as key facilitators in this endeavor. While the latter significantly utilizes the untapped spectrum of mmWave frequencies, the former makes extensive use of huge antenna arrays [1].

One of the most crucial methods utilized within mMIMO applications is transmit and receive beamforming (BF). Digital BF that processes the signals in the baseband has the advantage of generating accurate beams and streaming multiple signals simultaneously. On the other hand, analog BF achieves lower performance while providing much lower complexity and hardware/operational cost. This is explained by the fact that analog BF only requires a single radio-frequency (RF) chain with analog phase shifters and attenuators compared to the numerous RF chains equipped for digital BF. The trade-off among

these schemes has been extensively studied, and numerous hybrid beamforming techniques have been devised in the literature [2].

As analog BF becomes expensive for vast arrays, holographic beamforming (HBF) is a potential alternative that can be used in conjunction with massive MIMO and mmWave communication systems. The reconfigurable holographic surface (RHS), a metamaterial surface, is the essential component of HBF [3]. The main strength of HBF comes from the reduced cost of producing RHSs with a large number of metamaterial components [4], where the radiation power of each component can be controlled individually. Therefore, the primary distinction between HBF and other techniques is that the former only allows for the control of radiated wave amplitudes, while the latter allows for the control of phases as well as amplitudes. Furthermore, the term "holographic" refers to RHS physics, which shares many similarities with the holographic principle. RHSs can be built with several feeds, allowing for the implementation of digital BF and feeding its output to the RHS.

Compared to the current interest in HBF, the RHS design concept is comparatively more established [5]. From an antenna perspective, RHS is considered to be an array of leaky-wave antennas (LWAs). A reference wave is fed to the RHS from feeds and propagates along it. The LWAs leak this wave outside the surface, and beamforming is accomplished by regulating the amount of radiation from these elements. Numerous studies have been done on RHS operation and application cases [1, 3]. Recent research has placed a lot of attention on the multi-feed RHS, where methods are being developed to concurrently optimize the RHS weights and the digital beamformer for multi-user communication [6, 7]. However, the simple single-feed RHS and basic fully HBF are still in its infancy, and more studies on the subject of constrained optimization approaches for fully HBF are required.

Aside from HBF, directional modulation (DM) is a technique that utilizes antenna arrays to transmit digitally modulated symbols in a desired direction. It can be considered a special case of beamforming, where the purpose is not only to increase diversity and overcome the limitation of bad channel conditions but also to control the amplitudes and phases of transmitted signals in specific directions by means of beamformer weights. Its roots extend to 1990 [8], where the first directional binary phase-shift-keying (BPSK) was proposed by switching the transmitter antenna. The concept of delivering sinusoidal plane waves with different phases in time as a modulated signal was introduced. Two antennas were utilized with a distance equal to half the wavelength of the carrier frequency. Consequently, at the endfire of this 2-element array, the signal reaches with a 180° phase shift from the two antennas, and the BPSK is achieved by switching the active transmitting antenna at each symbol duration. The authors also proposed M-ary PSK by the same antenna switching mechanism using M-element array, where direction-dependent amplitude changes are achieved by appropriately selecting combinations of antennas.

Since that work, the concept of DM has been investigated intensively in different aspects [9]. As the number of studies related to large antenna arrays in communication systems increases, the DM concept becomes an important research area [10]. Starting with Antenna Subset Modulation (ASM) [11] and Switched Phased Array (SPA) [12] methods, the main focus has shifted toward utilizing this technique for physical layer

Table 1 A comparison between existed DM methods and the proposed work

	Phased array techniques	RIS-assisted works	Other BF approaches [15, 17]	This work
Purpose of the work	Security	Security [14] low-cost modulator [16]	Security	Low-cost modulator with security
Requiring modulated signal	No [11, 18] Yes [12]	No [16] yes [14]	Yes	No
Multi-user support	No	No	No	Yes

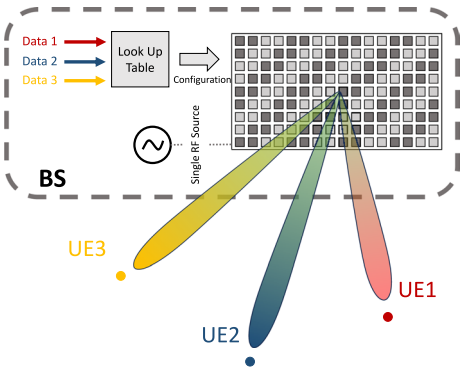

Fig. 1 Directional modulation with RHS. An illustration of the DM concept using RHS fed by a single unmodulated carrier

security. Recent works utilized reconfigurable intelligent surfaces (RISs), which are metasurfaces that share some common properties with RHS [13], to implement directional modulation for physical layer security. The authors in [14] focused on a single-user scenario with eavesdropper. By transmitting artificial noise and controlling the directions of the noise and the confidential messages, high secrecy rates were obtained. A new DM model was proposed in [15] utilizing hybrid beamforming. Improvements in secrecy rate and signal-to-interference-plus-noise ratio (SINR) were achieved with closed-form expressions. Another RIS-assisted DM system was presented in [16], where the signal is modulated in the RIS directly by the proposed time-domain digital coding approach. A detailed comparison of existing literature is listed in Table 1.

This paper proposes the concept of DM using RHS for simultaneously serving multiple users sharing the same frequency resources, as depicted in Fig. 1. Firstly, a mathematical model is developed to represent an in-phase/quadrature (IQ) sample as a sum of carriers, and an algorithm based on the mathematical model is constructed to generate the IQ samples toward specific directions using RHS. The main novelty of this work is the ability to support multi-user transmission using an unmodulated carrier generated by a single source within a RHS structure. This is a significant achievement as the single unmodulated carrier, together with the RHS with only on/off element states is utilized to produce a low-cost solution. Besides, the RF signal is obtained by only a local oscillator and amplifier, without requiring complex and expensive components such as digital-to-analog converters and mixers. The only

limitation of the proposed approach comes from the time required for switching the RHS elements from one configuration to another. With the advancement of metasurface prototyping, it is anticipated that the switching times would be sufficiently short [19, 20]. When there are multiple users in the system, unintended receivers observe the combined signals of all users as an arbitrary waveform, revealing a potential physical layer security application. The first set of experiments for a single user indicates that the modulator's accuracy increases as a larger RHS is utilized. In the second set of experiments for multiple users, error vector magnitude (EVM) results are reported for various user angular distances and RHS sizes. The results demonstrate that the modulator is able to convey information to two users at a small angular distance when the number of RHS elements is sufficiently high. Finally, the mutual information results of physical layer security experiments show that the proposed technique is highly reliable for future low-cost and secure spatially multiplexed communications.

The rest of this paper is organized as follows: Sect. 2 provides the proposed method, where first the mathematical bases for generating IQ samples from carriers are presented, and then the RHS impairments are added to the model and the DM algorithms are proposed. Performance measures and related numerical results are given in Sect. 3, and the paper is concluded with future research opportunities in Sect. 4.

2 Method

2.1 IQ sample formulation

A baseband IQ sample modulates the amplitude and phase of a carrier wave. Classical modulators take a local oscillator's wave as an in-phase component, shift it by $\pi/2$ *rad* to generate a quadrature component, multiply them with the real and imaginary parts of the baseband signal samples, and finally add up the two components. The result can be expressed as a sinusoidal wave with a specific amplitude and phase. In this section, it will be shown that this modulated signal can be generated by summing a large number of sinusoidals having consecutive small phase shifts. The sum of N sinusoidals with equal amplitudes is

$$x = \sum_{i=0}^{N-1} \sin(\omega_c t + \psi + id\psi), \tag{1}$$

where ω_c is a fixed carrier frequency, ψ is the initial carrier's phase, and $d\psi > 0$ is an arbitrary small phase difference. The summation can be expanded using Euler's formulas as

$$x = \frac{1}{2j} e^{j(\omega_c t+\psi)} \sum_{i=0}^{N-1} e^{jid\psi} - \frac{1}{2j} e^{-j(\omega_c t+\psi)} \sum_{i=0}^{N-1} e^{-jid\psi}. \tag{2}$$

The summations in eq. (2) can be calculated using the geometric series summation lemma, resulting in

$$x = \frac{1}{2j} e^{j(\omega_c t+\psi)} \frac{1-e^{jNd\psi}}{1-e^{jd\psi}} - \frac{1}{2j} e^{-j(\omega_c t+\psi)} \frac{1-e^{-jNd\psi}}{1-e^{-jd\psi}}, \tag{3}$$

which can be reduced to

$$x = \frac{\sin\left(\frac{N}{2}d\psi\right)}{\sin\left(\frac{d\psi}{2}\right)} \sin\left(\omega_c t + \psi + \frac{N-1}{2}d\psi\right). \tag{4}$$

Equation (4) states that, for a given $d\psi$, the phase of the resulting carrier depends on the initial phase (ψ) and the number of the sinusoidals (N). On the other hand, the amplitude depends only on N and the maximum amplitude is achieved when $Nd\psi = \pi$.

Thus, to modulate an IQ sample $s = s_R + js_i$ as a sum of sinusoidals, the sample is first converted to polar representation as $s = A_s e^{j\psi_s}$. The set of sinusoidals generating this symbol are chosen with N and ψ such that

$$N = 2\left\lceil \frac{\arcsin(A_s)}{d\psi} \right\rceil, \psi = \psi_s - \frac{N-1}{2}d\psi, \tag{5}$$

where $\lceil \cdot \rceil$ is the ceiling function used to obtain an integer number. Consequently, to modulate a complex symbol s, a series of N sinusoidal waves with $d\psi$ phase shifts starting from ψ is summed, where N and ψ are calculated as in Eq. (5). This approximation results in a quantization error that basically depends on $d\psi$ and its maximum values are calculated as

$$e_A = \frac{\sin d\psi}{2}, e_P = \frac{d\psi}{4}, \tag{6}$$

for the amplitude and phase, respectively.

A RHS with a high number of antenna elements radiates waves with numerous phase shifts. This means that a set of sinusoidals within the phase interval $[-\pi, \pi]$ can be obtained with small $d\psi$ separation. Consequently, to perform modulation in its simplest form, a set of sinusoidals is defined and the related RHS elements are switched on to radiate, while the other elements are switched off. This will be investigated in the next section.

2.2 Multi-user directional modulation for RHS

The previous section presents that IQ samples can be modulated by summing a set of sinusoidals having the same frequency with equal small phase shifts. The accuracy of this modulation is directly related to the phase shifts $d\psi$, which are assumed to be constant. In the far field of a RHS, the phases of radiated waves change according to the desired modulation angle, resulting in various phase shifts (i.e., $d\psi$ is not constant). In this section, the effect of these phase disruptions is investigated and a modulation algorithm is proposed to compensate it. In a given direction d defined by the (azimuth, elevation) (ϕ_d, θ_d) pair, the signal transmitted by the n^{th} RHS element is observed with a phase shift defined as [6]

$$\tau_{n,d} = e^{-jk_0(x_n \cos\phi_d + y_n \sin\phi_d)\sin\theta_d - jk_r|\boldsymbol{r_n}|}. \tag{7}$$

(x_n, y_n) in (7) represents the position of the RHS element, $\boldsymbol{r_n}$ is the vector from the RHS feed to the element, if the feed is in the center of the RHS then $\boldsymbol{r_n} = \sqrt{x_n^2 + y_n^2}$. k_0 and k_r are the wave numbers of free space and the dielectric of RHS, respectively. For the sake of simplicity, the coordinate system is referenced with respect to the RHS, so the z-axis is always perpendicular to the surface as illustrated in Fig. 2. A similar formulation can be made for the near field of the RHS, where the phase shifts depend on the location of the observation point instead of its direction. This can be beneficial especially when considering large RHSs where the near field might extend to multi-meters. However, it is left as a future work. Since there are a large number of elements in RHS, a variety of τ values is typically obtained. Without loss of generality, the waves radiated by RHS elements can be sorted and written in a series as the sinusoidal terms in eq. (1) with two differences as follows: each wave has a shared constant phase shift ($d\psi$) and element-dependent disruption (ϵ_i). Besides, some elements may have exactly the same phase, and this can be translated to a sinusoidal with higher amplitude (A_i). Consequently, performing the modulation of a symbol (s) is not as straightforward as in eq. (5). Instead, the set of sinusoidals will be chosen to cover all the waves within an interval centered at ψ_s and having a width of N elements relative to A_s. This is graphically illustrated in Fig. 3. The figure can be interpreted as a histogram of the obtained phase shifts at a given direction. As it can be seen in the figure, the amplitudes inside the defined interval are not exactly uniform, resulting in a disruption or modulation error. This error occurs in the phase and amplitude. However, it is quiet challenging to compensate this error for both, especially for multi-user communication scenario as will be shown later. For modulations such as phase shift keying (PSK), amplitude error is not as critical as phase error. Thus, an approach is first developed for PSK, where phase error correction is implemented.

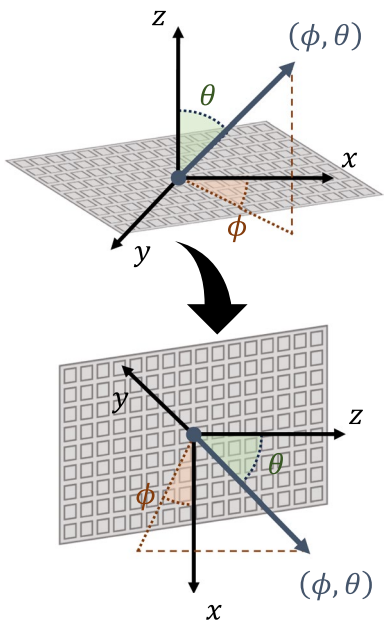

Fig. 2 The azimuth and elevation directions referenced by the RHS. The Cartesian coordinate system used through the paper and the resulting azimuth and elevation angles

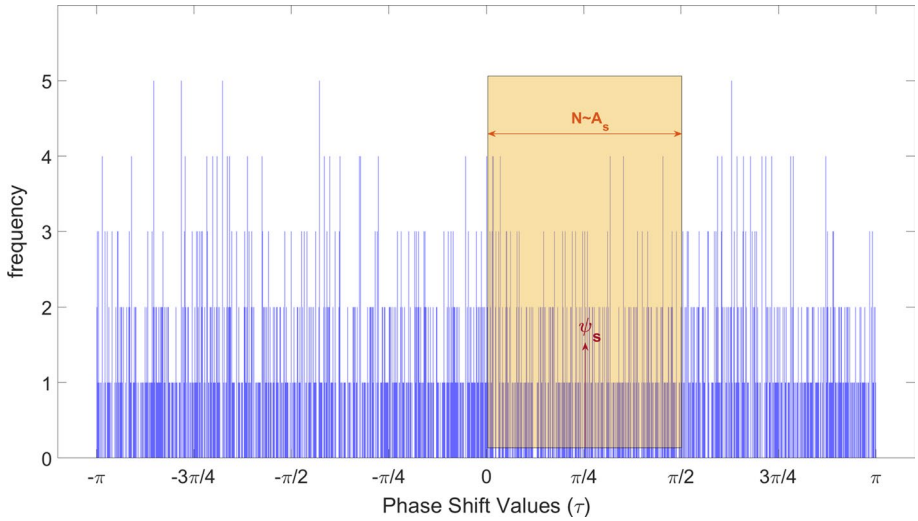

Fig. 3 Phase shifts distribution of a (40 × 40) RHS in a random direction. A histogram of the obtained phase shifts resulting from the elements of the RHS in a random direction. The rectangle shows how RHS element selection criteria to generate a specific IQ sample in this direction

2.2.1 Single-user PSK

Algorithm 1 shows the generation of a look-up table (LUT) for PSK modulation. For M-PSK and a specific user direction (ϕ_u, θ_u), the LUT holds M weight vectors ($\boldsymbol{w}$); each one is corresponding to a modulation symbol. The RHS fed by a carrier wave is then configured by switching the elements on or off according to the weight vector. The modulation is achieved by selecting elements within the interval of width π around the phase of the modulation symbol similar to Fig. 3. These elements are initially planned to transmit or switched to the on state. Then, in order to reduce the phase disruption, elements with highest or lowest phase shifts are excluded.

The algorithm takes a maximum error threshold ϵ for the phases of the modulated symbols. It iteratively excludes elements until reaching a phase error less than or equal to ϵ. This threshold controls the quality of the modulator and can be chosen to have very small values. However, these iterations also reduce the amplitude of the symbol. Although the main motivation to use PSK is to reduce the amplitude dependency, a limit $I_{\max}$ for the iterations (and hence a lower bound for the amplitude) needs to be defined. Depending on the number of RHS elements, the required quality may not be reached leading to amplitudes close to zero without this limit. For example, a 64-element RHS can generate, in the ideal case, a uniform distribution of phase shifts of 5.6 degrees. Thus, a phase threshold error of $\epsilon = 2$ degrees might be impossible to achieve and the algorithm will switch off all the elements trying to reach this threshold if $I_{\max}$ limit is not defined.

The vectors in line 5 are binary logical vectors and the product $(\circ)$ is element-wise multiplication. arg(.) gives the phase of a complex number and $(.)^T$ is the transpose operation. The performance of this modulator depends heavily on the number of RHS

elements and then on the direction of transmission. Although the trade-off between the phase and amplitude error is comprehensible, other modulations that carry information in the amplitude such as Quadrature Amplitude Modulation (QAM) can be realized for the single-user case with acceptable performance.

Algorithm 1 Single-User PSK

1: **Inputs:**
RHS, (θ_u, ϕ_u), M, ϵ, $I_{\max}$
2: **Initialize:**
Modulation Phases: $\psi_m = \frac{2\pi}{M} m, \;\; m = 0, 1, ..., M-1$
3: Calculate phase shifts vector $\boldsymbol{\tau}_u$ for all RHS elements
4: **for** $m = 0, 1, ..., M-1$ **do**
5: $\boldsymbol{w_m} = (\boldsymbol{\tau}_u \leq \psi_m + \pi/2) \circ (\boldsymbol{\tau}_u \geq \psi_m - \pi/2)$
6: $i = 0$
7: **while** $|\arg(\boldsymbol{\tau}_u^T \boldsymbol{w_m}) - \psi_m| > \epsilon$ **do**
8: $i++$
9: **if** $\arg(\boldsymbol{\tau}_u^T \boldsymbol{w_m}) > \psi_m$ **then**
10: remove the wave (q) with highest phase shift among active elements $w_{m,q} = 0$.
11: **else if** $\arg(\boldsymbol{\tau}_u^T \boldsymbol{w_m}) < \psi_m$ **then**
12: remove the wave (q) with lowest phase shift among active elements $w_{m,q} = 0$.
13: **end if**
14: **if** $i == I_{\max}$ **then**
15: break
16: **end if**
17: **end while**
18: $\text{LUT}(m,:) = \boldsymbol{w_m}$
19: **end for**
20: **Outputs:**
LUT

2.2.2 Single-user QAM

Algorithm 2 performs QAM modulation for a given direction. At the initialization step, all the amplitude values are normalized and multiplied with the maximum usable number of RHS elements, which is half of the total elements, as explained earlier. By this operation, half of the elements will be activated to transmit the highest amplitude, and this number will decrease relatively to the amplitudes of other symbols. Similar to Algorithm 1, a phase error correction routine is implemented (lines 7–11), but the purpose here is to reduce the number of active elements, and hence the amplitude, while maintaining a steady phase value.

Algorithm 2 Single-User QAM

Inputs:
RHS, (θ_u, ϕ_u), M
Initialize:
QAM Modulation Symbols: $s_m = A_m e^{j\psi_m}, \ \ i = 0, 1, ..., M$
Map different amplitude levels to different numbers of active RHS elements $A_m \rightarrow N_m$
Calculate phase shifts vector $\boldsymbol{\tau}_u$ for all RHS elements
for $m = 0, 1, ..., M$ **do**
  $\boldsymbol{w_m} = (\boldsymbol{\tau}_u \leq \psi_m + \pi/2) \circ (\boldsymbol{\tau}_u \geq \psi_m - \pi/2)$
  while $\sum_n w_{m,n} > N_m$ **do**
    if $\arg(\boldsymbol{\tau}_u^T \boldsymbol{w_m}) > \psi_m$ **then**
      remove the wave (q) with highest phase shift among active elements $w_{m,q} = 0$.
    else if $\arg(\boldsymbol{\tau}_u^T \boldsymbol{w_m}) < \psi_m$ **then**
      remove the wave (q) with lowest phase shift among active elements $w_{m,q} = 0$.
    end if
  end while
  $\text{LUT}(m,:) = \boldsymbol{w_m}$
end for
Outputs:
LUT

2.2.3 Multi-user PSK

The multi-user PSK modulation scheme is developed by utilizing Algorithm 1 separately for each user without phase error correction. The element-wise product of the resulting weight vectors is taken to find a weight vector activating only the common elements that satisfies all the users' desired phases. Due to the exclusion of the uncommon elements, the transmitted signals' amplitude degrades significantly and the phase errors increase. Thus, a minor error correction process with wave addition instead of removal is applied to improve the worst symbol of each modulation state. The error correction is limited by I_{max} which should take a relatively small value with respect to the number of RHS elements. From a communication perspective, these errors are considered as interference, since they arise and increase with the increasing number of users. The multi-user PSK directional modulator is introduced in Algorithm 3. A RHS configuration needs to be generated for each combination of different users' symbols. These symbol phase combinations are first calculated and stored in the matrix Ψ. The look-up table is then generated with entries for these states as illustrated.

Algorithm 3 Multi-User PSK

Inputs:
RHS, $\{(\theta_{u1}, \phi_{u1}), ..., (\theta_{uK}, \phi_{uK})\}$, M, $I_{\max}$
Initialize:
Modulation Phases: $\psi_m = \frac{2\pi}{M} m, \;\; m = 0, 1, ..., M-1$
Initialize:
States of Users' Symbol Combinations: Ψ matrix with M^K states.
Calculate phase shifts vectors $\boldsymbol{\tau}_{u,k}$ for all RHS elements
for $m = 1, ..., M^K$ **do**
  $\tilde{\boldsymbol{w}} = \mathbf{1}$
  for $k = 1, ..., K$ **do**
    $\tilde{\boldsymbol{w}} = (\boldsymbol{\tau}_{u,k} \leq \psi_{m,k} + \pi/2) \circ (\boldsymbol{\tau}_{u,k} \geq \psi_{m,k} - \pi/2) \circ \tilde{\boldsymbol{w}}$
  end for
  for $i = 1, ..., I_{\max}$ **do**
    Find user (k') with highest phase error
    if $\arg(\boldsymbol{\tau}_{u,k'}^T \tilde{\boldsymbol{w}}) > \psi_{m,k'}$ **then**
      add wave (q) with low phase shift among deactivated elements $\tilde{w_q} = 1$.
    else if $\arg(\boldsymbol{\tau}_{u,k'}^T \tilde{\boldsymbol{w}}) < \psi_{m,k'}$ **then**
      add wave (q) with high phase shift among deactivated elements $\tilde{w_q} = 1$.
    end if
  end for
  $\mathrm{LUT}(m,:) = \tilde{\boldsymbol{w}}$
end for
Outputs:
LUT

The multi-user PSK modulation in this study can be considered as a constrained optimization problem whose objective is to maximize the power of the signal in the desired directions. Since there are phase constraints depending on the desired user directions in addition to the constraint of the weight vector $\boldsymbol{w}$ to be real and binary, the proposed algorithm solves this complex problem.

3 Results and discussion

3.1 Complexity discussion

The proposed three algorithms assume the availability of prior information on the users' directions. The transmitter then calculates the look-up tables for these directions. While the look-up tables can be calculated previously for all possible directions with a certain resolution for the single-user case, this is not practically possible for the multi-user scenarios due to the infinite combinations of user directions. The complexity of the single-user algorithms changes linearly with the modulation order and the number of RHS elements, where the number of the look-up table entities and the calculated phase shifts changes, respectively. However, the complexity of the multi-user algorithm increases exponentially with the number of users as the number of their constellation symbol combinations increases exponentially. As a result, the single look-up table entity's complexity is not significantly affected by the number of users. Thus, a real-time implementation instead of the look-up table can be considered for large number of users, if an adequate computational capacity is available.

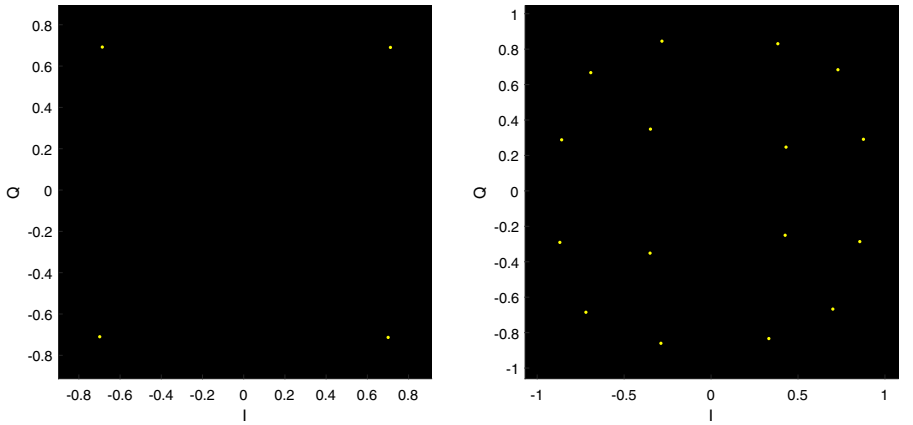

(a) Single-user QPSK.

(b) Single-user QAM.

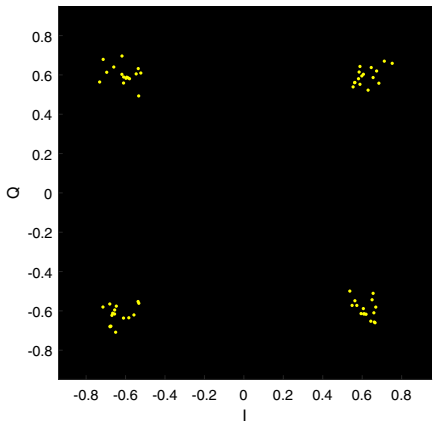

(c) 3-user QPSK (desired user).

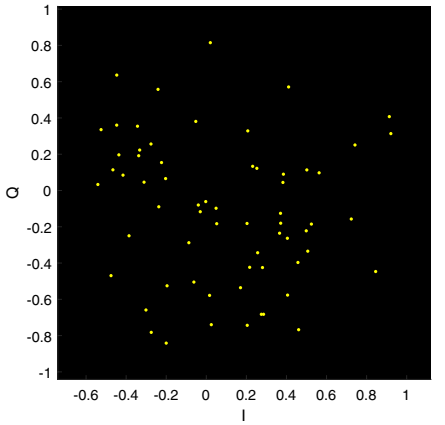

(d) 3-user QPSK (unintended user).

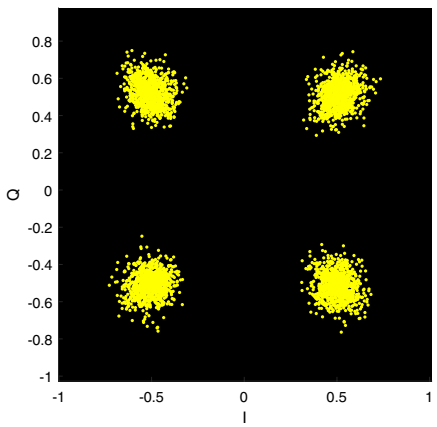

(e) 6-user QPSK (desired user).

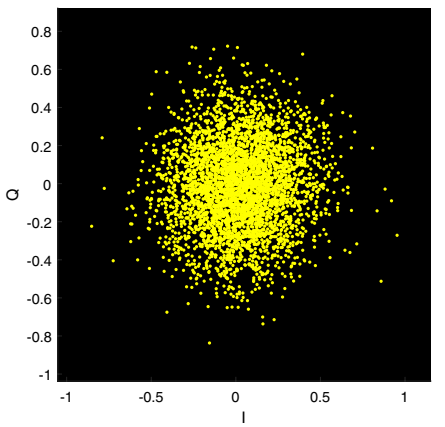

(f) 6-user QPSK (unintended user).

Fig. 4 Example constellation diagrams for the proposed modulator. The realized constellation diagrams of the DM algorithms. (**a**) Single-user QPSK, (**b**) single-user QAM, (**c**) a desired user's constellation in 3-user QPSK, (**d**) an unintended user's constellation in 3-user QPSK, (**e**) a desired user's constellation in 6-user QPSK, (**f**) an unintended user's constellation in 6-user QPSK

3.2 Performance measures

Figure 4 shows example constellations of the transmitted modulated signals. For a single-user PSK directional modulator, the purpose is to provide a constellation with a constant phase difference between each two consecutive symbols, independent from the total offset. Thus, the performance of the modulator for a given direction can be evaluated by observing the phase differences between consecutive modulation symbols. The average phase error for a direction u is calculated as

$$e_u = \frac{1}{M}\sum_{i=1}^{M} |\arg(\boldsymbol{\tau}_d^T \boldsymbol{w}_{\boldsymbol{mod}(\boldsymbol{i},\boldsymbol{M})}) - \arg(\boldsymbol{\tau}_d^T \boldsymbol{w}_{\boldsymbol{mod}(\boldsymbol{i-1},\boldsymbol{M})})|. \tag{8}$$

The second error measurement is the power deviation, which is merely the difference between the highest symbol's power and the lowest one. Moreover, since the modulation algorithm reduces the magnitude of total signal while correcting the phase error, the power efficiency of the modulator across different directions needs to be considered. As stated in eq. (4), the maximum signal amplitude is achieved by observing sinusoidals with phases in an interval of π width. Consequently, a perfect modulator with a uniform distribution of phase shifts will have at most half of its total available waves in this interval to utilize. This upper limit can be taken as a reference for the power efficiency of the PSK directional modulator. Power efficiency refers to the ratio of the radiated power to the fed power. While this quantity requires complicated electromagnetic radiation calculations, it will be assumed as the number of active elements divided by the total number of elements. Hence, the maximum achieved power efficiency is 50%, and the minimum is

$$\eta\% = \frac{N/2 - I_{\max}}{N} \times 100. \tag{9}$$

The performance measurement in multi-user case will be the EVM at the transmitter's output. The reason is that each symbol s_i of a user may be generated with different 2^{K-1} errors related to the combinations of the other $(K-1)$ users' symbols. Since these errors are sourced from other users information, they can be considered as interference. For the physical layer security of the multi-user modulator, the mutual information is used as the performance measurement. It is not possible to evaluate the secrecy rate since the signal may not be necessarily suppressed in undesired directions.

3.3 Single-user modulator's performance

In this section, simulation results for a single-user modulator are presented. Figure 5 shows the change in performance metrics of a single-user modulation with the size of the RHS. The RHS is assumed to be a square of $\sqrt{N_{\text{RHS}}} \times \sqrt{N_{\text{RHS}}}$ elements. For each N_{RHS} value, the 8-PSK configuration look-up table is generated for all the pairs of (azimuth, elevation) within $([0, 180], [-90, 90])$ intervals, respectively. The mean of phase error and power variation among the whole plane is then recorded and plotted. The mean power variations are around 2.74dB and 0.13dB, and the mean phase errors are around 1.21 and 0.01 degrees for 64-element and 6400-element RHSs, respectively. Both metrics exponentially decreases as the number of RHS elements

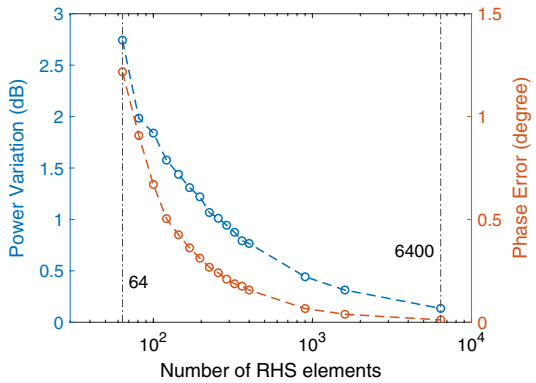

Fig. 5 The performance of the single-user modulator against the size of RHS. Mean power variation and phase error changes with RHS sizes. The mean is taken over all the (azimuth,elevation) plane

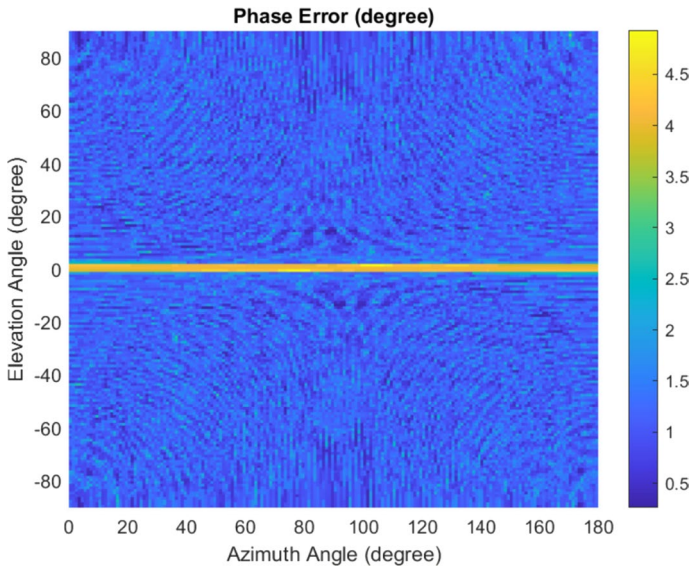

Fig. 6 Single-user modulator's performance in different directions for an 8×8 RHS. The phase error distribution of a single-user QPSK modulator over the (azimuth,elevation) plane

increases. The results confirm that larger RHS yields more accurate modulators with less phase and amplitude errors. It is important to remind that the performance is not affected by the modulation order, since higher modulation orders imply only generating new RHS configurations with the same phase error profile.

Two parameters, namely the error threshold and the maximum number of iterations, in Algorithm 1 need to be tuned to balance the trade-off between the phase error and the power efficiency. Reducing the error threshold or increasing the maximum number of iterations provides the desired improvement in the phase error at the expense of the power efficiency. An important point to consider is that the performance degrades significantly at certain directions, specifically, in the perpendicular direction of the RHS. These phenomena are expected, since at this direction, the phase differences among neighbored RHS elements are negligibly small. This is

visualized in Fig. 6, where the error distribution on the azimuth/elevation plane is plotted.

3.4 Multi-user modulator's performance

In the multi-user case, the performance is affected by

- The number of RHS elements,
- The number of users,
- The angular distance between users.

A simulation of three users with QPSK is conducted. The first user has a fixed direction among all simulations at (45, 30) degrees for (azimuth, elevation), respectively, and named as the far user. The second user is at a relatively separate direction with respect to the far user and is named as the reference user. The term "far" here indicates the angular distance between the two users. The third user is located at different directions that are relatively close to the reference user; hence, it is called the moving user. The reference user's direction is altered 5 times, and for each direction, the moving user's direction is altered to have 10 different directions on a circle of angular distance d. The performance is then evaluated for different angular distances as illustrated in Fig. 7. The simulation results in terms of EVM are shown in Fig. 8. Note that each point in Fig. 8 is obtained as the mean of 50 simulations (5 different directions for the reference user and 10 different directions for the moving user). Suppose that there is an EVM threshold value defining a "good" modulation, then it can be concluded from the figure that the minimum angular distance satisfying a good modulation decreases when the number of RHS elements increases. Furthermore, for a RHS with 6400 elements, an EVM of 7.2% is achieved with an angular separation of 5 degrees between the reference and moving users. As the angular separation is 20 degrees, the EVM value drops to 2.6%. It can also be seen that the performance of the far user remains constant beyond a certain angular distance depending on the number of RHS elements. For example, for the 6400-element RHS, the far user's EVM is around 2.6% when the angular distance between the other users is greater than 5 degrees. On the other hand, for the 400-element RHS, the far user's EVM is between

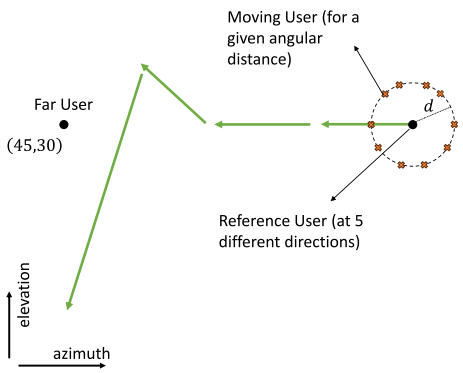

Fig. 7 The simulation scenarios for multi-user directional modulation. The far user is located at a fixed direction, the reference and the moving users change directions as illustrated

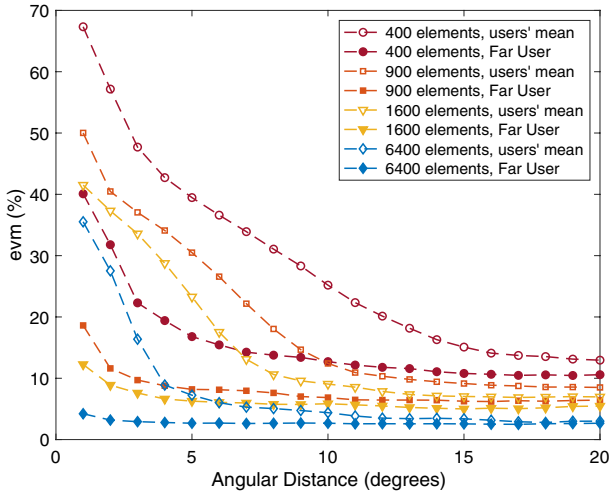

Fig. 8 The performance of multi-user directional modulation. EVM vs the angular separation between the reference and moving users for different RHS sizes is shown

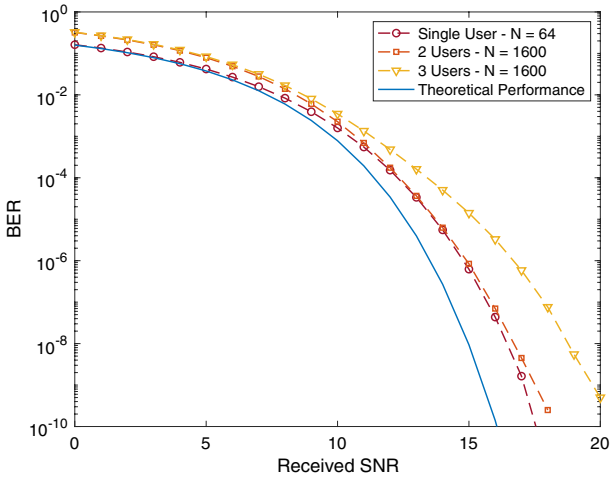

Fig. 9 The BER performance of the proposed modulator. BER vs received SNR is shown for different number of users with theoretical limit

11.06% and 10.47% when the angular distance between the other users increases from 14 to 20 degrees. It is important to note that when the angular distance between the other users is low, the EVM of the far user becomes higher. This is because of the min-max behavior of the algorithm that disrupts the far user's symbols while trying to improve the symbols of the reference and moving users.

Another important performance metric is the bit error rate (BER) which is shown with respect to the received signal-to-noise ratio (SNR) in Fig. 9. While the QPSK SU modulator exhibits a performance close to the theoretical limits, the trade-off with the increasing number of users is clearly shown. Finally, to evaluate the mutual information, a modulator with 6 desired user directions is simulated. A 40×40 RHS is used and the output of the modulator is observed among the whole azimuth/elevation plane. This

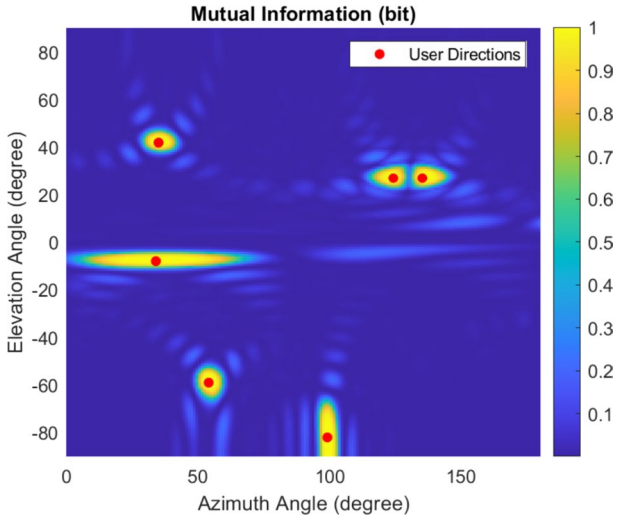

Fig. 10 Mutual information for 6-user scenario with 40 × 40 RHS. Each point in the plane represents the highest mutual information between the received signal at that point and the six users' data

scenario utilizes QPSK modulation resulting in a LUT with 2^{12} states, where each state defines a 12-bit combination for the 6 users. To consider all possible combinations, a sequence of 2^{13} bits is transmitted for each user. Hence, at each direction, the mutual information between demodulated symbols and each of the original user bit sequences is calculated and the maximum value is recorded. Figure 10 shows the maximum mutual information values. The results are promising as the information is spread only over a limited region around the intended user. However, some directions have slightly higher information leakage like those close to 0 and − 90 directions in the elevation axis. This happens because the phase shifts of the RHS elements at these directions do not exhibit sufficient variations. It is not possible to achieve this kind of information security if the unintended user is in the same direction of an intended user. However, utilizing near-field communication is a promising solution for this problem as it is location-dependent.

4 Conclusion

This paper introduces multi-user directional modulation for reconfigurable holographic surfaces fed by a single-carrier wave. We propose a codebook-based directional modulation algorithms to configure the states of the RHS elements. A set of simulation experiments has been conducted to investigate the performance of the modulator. The results show that the proposed approach enables serving multiple users at the same time and frequency resources by spatially diverging their separated symbols. Future works will perform experimental verification using real hardware. In addition, multi-feed RHS, multi-state RHS elements, and various waveforms will be investigated to improve the modulator's accuracy.

Abbreviations

6G	Sixth Generation
ASM	Antenna Subset Modulation
BER	Bit Error Rate
BPSK	Binary Phase Shift Keying

BF	Beamforming
DM	Directional Modulation
EVM	Error Vector Magnitude
HBF	Holographic Beamforming
IQ	In-Phase/Quadrature
LUT	Look-up Table
LWA	Leaky-wave Antenna
MIMO	Multiple Input Multiple Output
mMIMO	Massive Multiple Input Multiple Output
mmWave	Millimeter Wave
PSK	Phase Shift Keying
QAM	Quadrature Amplitude Modulation
RF	Radio-Frequency
RHS	Reconfigurable Holographic Surface
RIS	Reconfigurable Intelligent Surface
SINR	Signal-to-Interference-Plus-Noise Ratio
SINR	Signal-to-Noise Ratio
SPA	Switched Phased Array

Acknowledgements
We thank to StorAIge project that has received funding from the KDT Joint Undertaking (JU) under Grant Agreement No. 101007321. The JU receives support from the European Union's Horizon 2020 Research and Innovation Programme in France, Belgium, Czech Republic, Germany, Italy, Sweden, Switzerland, Türkiye, and National Authority TÜBİTAK with project ID 121N350.

Author contributions
The authors contributed equally to this work. All authors read and approved the final manuscript.

Funding
There is no funding to report.

Availability of data and materials
Data sharing is not applicable to this article as no datasets were generated or analyzed during the current study.

Declarations

Competing interests
The authors declare that they have no conflict of interest.

Received: 20 November 2023 Accepted: 28 June 2024
Published online: 11 July 2024

References

1. T. Gong, P. Gavriilidis, R. Ji, C. Huang, G.C. Alexandropoulos, L. Wei, Z. Zhang, M. Debbah, H.V. Poor, C. Yuen, Holographic mimo communications: theoretical foundations, enabling technologies, and future directions. IEEE Commun. Surv. Tutor. **26**(1), 196–257 (2024). https://doi.org/10.1109/COMST.2023.3309529
2. I. Ahmed, H. Khammari, A. Shahid, A. Musa, K.S. Kim, E. De Poorter, I. Moerman, A survey on hybrid beamforming techniques in 5g: architecture and system model perspectives. IEEE Commun. Surv. Tutor. **20**(4), 3060–3097 (2018). https://doi.org/10.1109/COMST.2018.2843719
3. R. Deng, B. Di, H. Zhang, D. Niyato, Z. Han, H.V. Poor, L. Song, Reconfigurable holographic surfaces for future wireless communications. IEEE Wirel. Commun. **28**(6), 126–131 (2021). https://doi.org/10.1109/MWC.001.2100204
4. C. Huang, S. Hu, G.C. Alexandropoulos, A. Zappone, C. Yuen, R. Zhang, M.D. Renzo, M. Debbah, Holographic mimo surfaces for 6g wireless networks: opportunities, challenges, and trends. IEEE Wirel. Commun. **27**(5), 118–125 (2020). https://doi.org/10.1109/MWC.001.1900534
5. D.R. Smith, O. Yurduseven, L.P. Mancera, P. Bowen, N.B. Kundtz, Analysis of a waveguide-fed metasurface antenna. Phys. Rev. Appl. **8**, 054048 (2017). https://doi.org/10.1103/PhysRevApplied.8.054048
6. R. Deng, B. Di, H. Zhang, Y. Tan, L. Song, Reconfigurable holographic surface: holographic beamforming for metasurface-aided wireless communications. IEEE Trans. Veh. Technol. **70**(6), 6255–6259 (2021). https://doi.org/10.1109/TVT.2021.3079465
7. B. Di, Reconfigurable holographic metasurface aided wideband ofdm communications against beam squint. IEEE Trans. Veh. Technol. **70**(5), 5099–5103 (2021). https://doi.org/10.1109/TVT.2021.3070361
8. E.J. Baghdady, Directional signal modulation by means of switched spaced antennas. IEEE Trans. Commun. **38**(4), 399–403 (1990). https://doi.org/10.1109/26.52647
9. O. Ansari, M. Amin, Directional modulation techniques for secure wireless communication: a comprehensive survey. EURASIP J. Wirel. Commun. Netw. **2022**(1), 93 (2022). https://doi.org/10.1186/s13638-022-02175-7
10. M.P. Daly, J.T. Bernhard, Directional modulation technique for phased arrays. IEEE Trans. Antennas Propag. **57**(9), 2633–2640 (2009). https://doi.org/10.1109/TAP.2009.2027047
11. N. Valliappan, A. Lozano, R.W. Heath, Antenna subset modulation for secure millimeter-wave wireless communication. IEEE Trans. Commun. **61**(8), 3231–3245 (2013). https://doi.org/10.1109/TCOMM.2013.061013.120459

12. N.N. Alotaibi, K.A. Hamdi, Switched phased-array transmission architecture for secure millimeter-wave wireless communication. IEEE Trans. Commun. **64**(3), 1303–1312 (2016). https://doi.org/10.1109/TCOMM.2016.2519403
13. Y. Liu, X. Liu, X. Mu, T. Hou, J. Xu, M. Di Renzo, N. Al-Dhahir, Reconfigurable intelligent surfaces: principles and opportunities. IEEE Commun. Surv. Tutor. **23**(3), 1546–1577 (2021). https://doi.org/10.1109/COMST.2021.3077737
14. R. Dong, S. Jiang, X. Hua, Y. Teng, F. Shu, J. Wang, Low-complexity joint phase adjustment and receive beamforming for directional modulation networks via IRS. IEEE Open J. Commun. Soc. **3**, 1234–1243 (2022). https://doi.org/10.1109/OJCOMS.2022.3195050
15. R. Dong, B. Shi, X. Zhan, F. Shu, J. Wang, Performance analysis of massive hybrid directional modulation with mixed phase shifters. IEEE Trans. Veh. Technol. **71**(5), 5604–5608 (2022). https://doi.org/10.1109/TVT.2022.3152807
16. J.Y. Dai, W. Tang, L.X. Yang, X. Li, M.Z. Chen, J.C. Ke, Q. Cheng, S. Jin, T.J. Cui, Realization of multi-modulation schemes for wireless communication by time-domain digital coding metasurface. IEEE Trans. Antennas Propag. **68**(3), 1618–1627 (2020). https://doi.org/10.1109/TAP.2019.2952460
17. F. Shu, X. Wu, J. Hu, J. Li, R. Chen, J. Wang, Secure and precise wireless transmission for random-subcarrier-selection-based directional modulation transmit antenna array. IEEE J. Sel. Areas Commun. **36**(4), 890–904 (2018). https://doi.org/10.1109/JSAC.2018.2824231
18. B. Zhang, W. Liu, J. Ma, Z. Qi, J. Zhang, L. Han, Y. Li, X. Zhao, C. Zhang, C. Wang, Sparse antenna array based positional modulation design with a low-complexity metasurface. IEEE Access **8**, 177640–177646 (2020). https://doi.org/10.1109/ACCESS.2020.3027285
19. J. Shabanpour, Programmable anisotropic digital metasurface for independent manipulation of dual-polarized thz waves based on a voltage-controlled phase transition of vo 2 microwires. J. Mater. Chem. C **8**(21), 7189–7199 (2020). https://doi.org/10.1039/D0TC00689K
20. K. Zangeneh Kamali, L. Xu, N. Gagrani, H.H. Tan, C. Jagadish, A. Miroshnichenko, D. Neshev, M. Rahmani, Electrically programmable solid-state metasurfaces via flash localised heating. Light: Sci. Appl. **12**(1), 40 (2023). https://doi.org/10.1038/s41377-023-01078-6

Publisher's Note